IV.I.10 Thermodynamics and Kinetics of Phase Transformations in Hydrogen Storage Materials

PI: Gerbrand Ceder, Co-PI: Nicola Marzari
Department of Materials Science & Engineering, Massachusetts Institute of Technology

Co-PI: Vidvuds Ozolins
Department of Materials Science & Engineering, University of California, Los Angeles

Contract Number: DE-FG02-05ER46253

Date of report: April 24, 2009
Period covered by the report: January 2008 – April 2009

Accomplishments

Reaction Kinetics and Dynamical Properties of Complex Hydrides

We have achieved significant progress in understanding fundamental atomic-scale mechanisms of phase transformations and mass transport in hydrogen storage materials. The activation energy for bulk Na diffusion via NaH vacancies is found to be significantly higher, Q=112 kJ/mol H_2 (see Figure 1). Achievements are as follows:

- Showed that the calculated activation energy for AlH_3 vacancy diffusion in $NaAlH_4$ is 85 kJ/mol H_2, suggesting that it is the rate-limiting step in hydrogen release kinetics from Ti-doped samples.

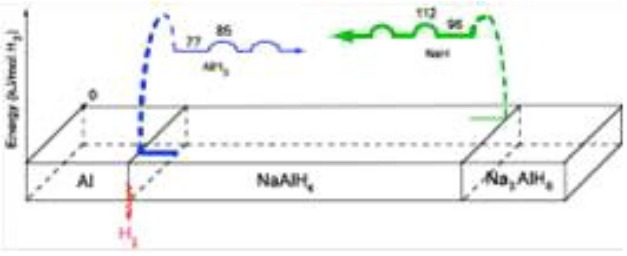

FIGURE 1. Proposed energy profile for the dehydrogenation pathway of $NaAlH_4$ via AlH_3 vacancies (blue curve). AlH_3 vacancies are created at the surface or at the Al/$NaAlH_4$ interface and diffuse towards $NaAlH_4$/Na_3AlH_6 interface, where they are annihilated by forming Na_3AlH_6. The diffusion of NaH vacancies requires a higher activation barrier and is unfavorable. Dashed lines correspond to unknown energy barriers associated with the nucleation of product phases and interfacial reactions.

- Obtained the activation energies for surface-controlled vacancy creation in pure undoped $NaAlH_4$, showed that vacancy creation limits the dehydrogenation kinetics for particle sizes above ~0.1 μm.
- Identified a novel (γ) phase for $NaAlH_4$, stable at room temperature, which is an intermediate transient in the dehydrogenation reaction.
- Studied H diffusion in the presence of NaH, AlH_3, H^0, and H^- vacancies in bulk $NaAlH_4$, H^0, and H^- interstitials in bulk $NaAlH_4$, and an H^- vacancy in a (001) surface slab.
- Developed a first-principles theory of H diffusion in Al in the presence of defects.

In sodium alanate, and most other modern hydrogen storage materials, H_2 release and uptake reactions are accompanied by long-range diffusion of metal species. Using density-functional theory (DFT) molecular dynamics simulations and the potential mean force umbrella sampling approach, we have previously obtained the activation energy for Al mass transport via neutral AlH_3 vacancies, Q=85 kJ/mol H_2. This value is in excellent agreement with the experimentally measured activation energies in Ti-catalyzed $NaAlH_4$ of around 80 kJ/mol H_2. *Our results suggest that bulk diffusion of Al species is the rate-limiting step in the dehydrogenation of Ti-doped samples of $NaAlH_4$.* The calculated diffusion coefficient and vacancy concentration at typical decomposition temperatures (D=4 ×10-4 cm^2/s and CV=0.01% at 400 K, respectively) are consistent with the observed dehydrogenation times of minutes to hours in ball-milled Ti-doped powders consisting of micron-sized grains. This study showed that Ti doping is not needed to obtain bulk mass transport at rates that are consistent with the observed dehydrogenation kinetics, and therefore the catalytic effect of Ti is not related to accelerated bulk diffusion. Since the measured activation energy in pure $NaAlH_4$ (118 kJ/mol H_2) is higher than our calculated activation energy for bulk diffusion of Al, hydrogen release from undoped $NaAlH_4$ is not limited by bulk diffusion, but could be controlled by surface or interfacial reactions. We have further refined our earlier calculations and investigated the possibility that the process of breaking an Al-H bond and creating a vacancy at the surface or at a multiphase interface (e.g., Al/$NaAlH_4$) is the rate-limiting step. The results of this study are shown in Figure 2. Using the generalized gradient approximation (GGA), we find that the generation of AlH_3 vacancies at the (001) surface requires an activation enthalpy of 96 kJ/mol H_2. The competing

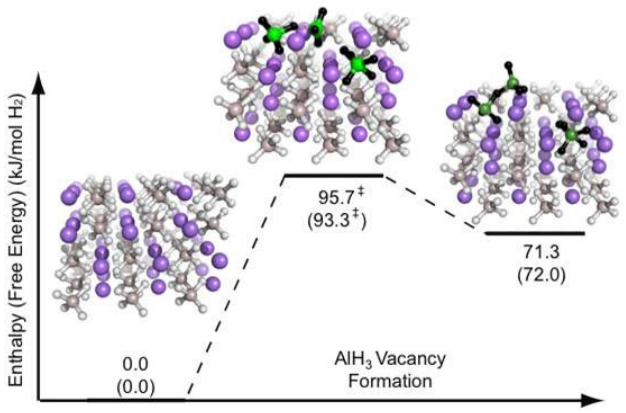

FIGURE 2. Zero-point energy corrected electronic energies and the structure of the transition state (marked by ‡) for creating charge-neutral AlH_3 and NaH vacancies at the (001) surface of sodium alanate. Al, H and Na atoms are shown as gray, white and purple spheres, respectively. Al atoms that are changing their bonding environments during the reactions are colored green, and H atoms that are attached to these Al atoms are colored black. The surface Na+ ion obtained upon forming the NaH vacancy is blue.

diffusion pathway via the creation of NaH vacancies was found to require 130 kJ/mol H_2 at the (001) surface, significantly higher than that required for the AlH_3 vacancy process. More accurate quantum chemistry calculations at the CBS-QB3 level for the activation enthalpy of breaking the Al-H bond, $AlH_4^- \rightarrow AlH_3 + H^-$, show that the DFT tends to underestimate the Al-H bond enthalpies by 24 kJ/(mol H_2). The corrected activation barrier, 120 kJ/mol H_2, is higher than the computed bulk diffusion barrier (85 kJ/mol H_2), and agrees very well with the experimental data for undoped $NaAlH_4$, indicating that vacancy creation is indeed be the rate-limiting step in pure $NaAlH_4$. We have computed the critical particle size where crossover from bulk-diffusion dominated kinetics to surface vacancy-creation dominated kinetics occurs. We find that *for particle sizes on the order of 0.1 μm and above, the surface vacancy creation is the rate-limiting process for dehydrogenation, and therefore one of the catalytic functions of Ti is to facilitate the breaking of Al-H bond*

We have also been performing extensive studies of the dehydrogenation of $NaAlH_4$ using total energy and total free energy calculations, linear-response theory, and first-principles molecular dynamics. We take this material as a paradigmatic example for what insight simulations can give on the thermodynamics and kinetics of the reaction – in addition, despite a wealth of recent, the precise mechanism of dehydrogenation, as well as the role of the dopants (e.g. titanium) in enhancing the reaction chemistry, remains unknown. Moreover, given the complexity of the configurational phase space and the difficulty of isolating dominant reaction pathways, it is unlikely that static energetic calculations will ever be fully capable of capturing the reaction kinetics. We have focused on the first dehydrogenation reaction ($NaAlH_4 \rightarrow 1/3\ Na_3AlH_6 + 2/3\ Al + H_2$), which is thought to be more useful under actual operating conditions. The key result is our *discovery of a novel phase, thermodynamically more stable than the reactant alanate at temperatures greater than 250 K, that bears a striking topological similarity with the end product Na_3AlH_6, and whose vibrational signatures are in agreement with recent experimental observations.*

In Figure 3, we present the structure of this new phase of $NaAlH_4$, which we will designate as γ. When relaxed with respect to all internal parameters and lattice vectors, the unit cell is best described as a 12-atom base-centred orthorhombic structure, with a = 6.652 Å, b = 7.235 Å, and c = 7.243 Å. We compared the total energy of this new structure, calculated using 216 **k**-points, to that of the ground-state α phase, calculated using a 324-**k** point mesh of similar density. At 0 K, the α phase is more stable energetically by only 8 meV/atom, pointing to a close competition for stability between these two phases. In order to establish finite-temperature properties, we have calculated the phonon dispersions for the α and γ phases using density-functional perturbation theory. shows the results of this calculation along high-symmetry directions in the orthorhombic unit cell of γ-$NaAlH_4$ (results for α-$NaAlH_4$ are not explicitly shown but are in close agreement with published results). Phonon bands below 180 cm-1 represent the Na/Al translational lattice modes; bands in the 180–400 cm-1 range represent the AlH_4 rotational modes; and bands in the 750–900 cm^{-1} range represent the Al–H bending modes. High-frequency Al–H stretching modes (1,650–1,820 cm^{-1}) are not depicted. Figure 4(c) points to the essential qualitative difference between the phonon dispersions of the two phases: the bands corresponding to the AlH_4 rotational

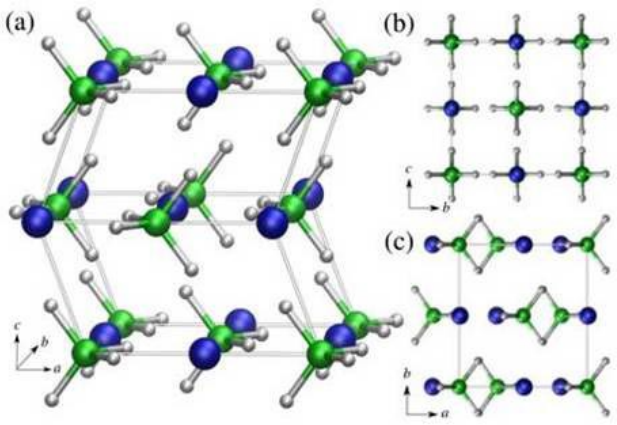

FIGURE 3. Structure of orthorhombic γ-NaAlH4 shown (a) in the standard view; (b) along a, and (c) along c. Na atoms are shown in blue, Al in green, and H in white.

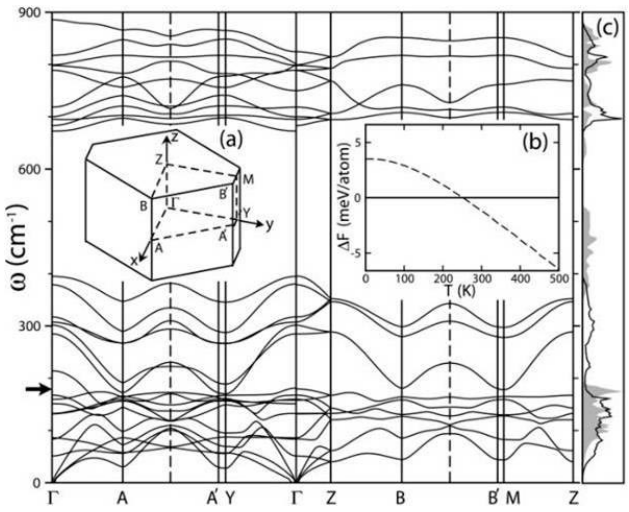

FIGURE 4. Phonon spectrum of γ-$NaAlH_4$ along the high-symmetry directions depicted in (a). Frequencies above 900 cm^{-1} are not shown. The solid arrow indicates the highest frequency of occupied bands at the α→γ transition temperature. Inset (b) shows the temperature-dependent free-energy difference between the two phases. Panel (c) compares the phonon densities of states for the γ phase (solid line) and the α phase (shaded region).

modes, which fall in the 350–550 cm^{-1} range for the α phase, are substantially softened in the γ phase. This softening results in an increase in vibrational entropy at temperatures for which these modes are active. We estimate the temperature-dependent free energy *F(T)* of the two phases by adding the Bose-Einstein vibrational entropy contribution onto the ground-state total energy. Neglecting further contributions to *F(T)*, we find a thermodynamic preference for the γ phase over the α phase for temperatures above 252 K (see Figure 4(b)). Notably, this establishes the γ phase as the most stable variant within the experimental temperature range for dehydrogenation. In a recent in situ Raman study, Yukawa et al. (J. Alloys Comp. 446-447, 242 (2007)) found evidence of an unknown intermediate phase in first-stage dehydrogenation. The authors suggest that, like our proposed γ phase, this new phase is stable at room temperature and contains intact AlH_4 units with little constraint from the crystal lattice. Accompanying this intermediate, they record the emergence of a new signature vibrational peak for Al--H stretching near 1,800 cm^{-1}. While absent for α $NaAlH_4$, this peak is clearly manifest in our calculated phonon density of states for γ, making the latter a likely candidate for the unidentified phase.

Hydrogen Kinetics in Aluminum

Measuring the diffusion rate of hydrogen in metals is important for understanding the kinetics of hydrogen storage, hydrogen-induced deterioration in the mechanical properties (e.g. embrittlement and cracking) and electrochemical charging of metals. However, a consensus on the physical mechanisms and numerical values of H diffusion coefficients in metals is still lacking. Even in the widely studied case of H in Al, published experimental measurements of the activation enthalpy and pre-exponential factor range from 0.17 to 0.94 eV and from 10^{-1} to 10^{-4} cm^2/s, respectively. Disparity in the measured rates is often attributed to the difficulties in measuring H diffusion accurately due to low solubility of H in Al and due to binding of H to structural defects. Based on the results of earlier first-principles calculations, we have developed a quantitative theory of hydrogen diffusion in aluminum with lattice defects. *Ab initio* molecular dynamics simulations have been used to obtain the activation energy and prefactor for lattice diffusion of H in Al between 650 and 850 K: $\Delta H^{\ddagger}$=0.12 ± 0.02 eV and D_0=1.1×10^{-7} m^2/s. Vacancies are found to significantly decrease the apparent diffusivity due to their ability to bind hydrogen atoms, causing a strong composition-dependence and non-Arrhenius behavior of the effective diffusion coefficient. The effective experimentally measured diffusion coefficient is given by the following expression:

$$D = D_L \Big/ \left(1 + \frac{\partial C_{\text{trap}}}{\partial C_L}\right)$$

which depends on the hydrogen concentration in the lattice (C_L) and trap (C_{trap}) sites. Hydrogen exchange between the lattice and vacancies leads to an apparent reduction in the diffusion coefficient, explaining the wide disparities in the measured activation energies and prefactors (see Figure 5). Finally, we show that an earlier suggestion by Lu and Kaxiras [Phys. Rev. Lett. **94**, 155501 (2005)] that up to twelve hydrogen atoms may get trapped in one vacancy, is not expected to occur

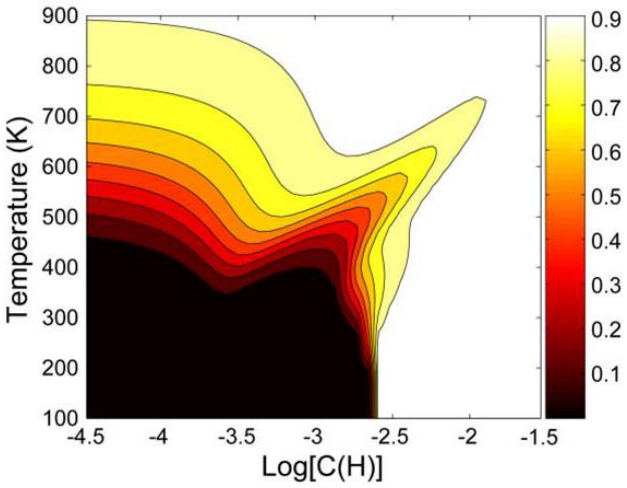

FIGURE 5. Calculated correction factor to the apparent diffusion coefficient, $(1 + \partial C_{\text{trap}}/\partial C_L)^{-1}$ as a function T and C_H.

at reasonable temperatures and hydrogen pressures (Figure 6).

Nano-Scale Effects on the Thermodynamics and Structure of Hydrogen Storage Materials

In previous years we focused on predicting the structure and thermodynamics of hydrogen storage materials. This year we initiated our study of the size effects on the structure and thermodynamics of hydrogen storage materials. Dealing with nanomaterials is considerably more complex than with bulk materials as there are no periodic boundary conditions and the role of the surfaces is crucial. Towards the objective of understanding nanomaterials we achieved the following results:

- Developed novel cluster expansion techniques to predict atomic ordering and structure of nanoparticles.
- Applied the new approach to sodium alanate ($NaAlH_4$) to predict the shape of small nanoparticles of this material.

Sodium alanate is a widely-studied hydrogen storage material, with a theoretical gravimetric capacity of 5.6%. Bulk sodium alanate releases hydrogen at temperatures well above 100°C, which is too high for use in PEM fuel cells. However it has recently been shown that 2-10 nm sodium alanate nanoparticles release hydrogen at a peak temperature of 70°C, which is within the target range for PEM fuel cells. The activation energy for hydrogen release in nanoparticles is significantly lower than the bulk activation energy for reasons that remain unknown.

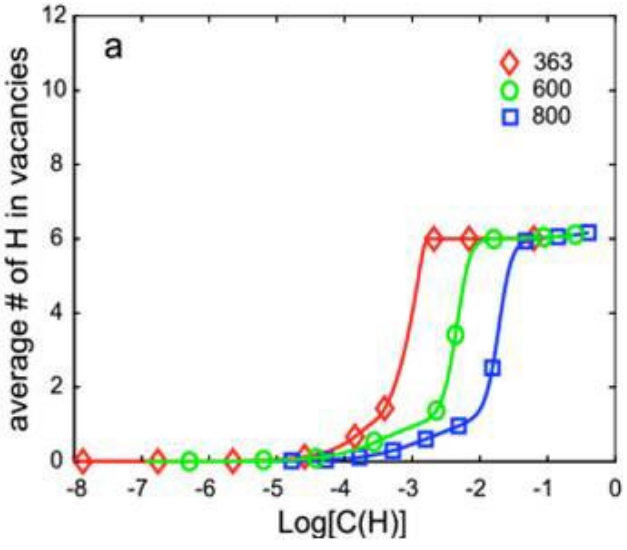

FIGURE 6. Left: average number of H atoms per vacancy, n_V, as function of the total hydrogen concentration. Red, blue and green curves represent T=363, 600, and 800 K, respectively.

The morphology of $NaAlH_4$ nanoparticles may play a significant role in lowering the activation energy for hydrogen release, but determining the shape of nanoparticles is both experimentally and computationally challenging. A common method for determining equilibrium particle shape is the Wulff construction, in which the distance between the center of the particle and a (*lmn*) surface facet is proportional to the bulk (*lmn*) surface energy. However, because the Wulff construction assumes large surfaces and ignores edges, vertices, and size effects, it is better suited for large particles than 2-10 nm nanoparticles. In addition, the Wulff construction requires that the complete set of relevant surfaces is already known. As an alternative to the Wulff construction, we have developed a cluster expansion. Hamiltonian trained on density functional theory calculations that enables us to rapidly and accurately calculate the energy of a particle with a given shape. Using the cluster expansion, we are able to predict the shape of $NaAlH_4$ nanoparticles by directly searching for the shape with the lowest energy. This approach naturally incorporates edge and vertex effects and allows the determination of particle shapes without *a-priori* knowledge of the important surfaces. In Figure 7, we show the difference between the shape predicted by a Wulff construction and the shape predicted by the cluster expansion for a sodium alanate nanoparticle that is about 6 nanometers wide.

The cluster expansion approach reveals new surfaces and sites that may be keys to understanding the enhanced activity of $NaAlH_4$ nanoparticles. For example, the (116) surface of sodium alanate is not close-packed and was not considered as a potential low-energy surface in previous studies [6,7]. However nanoparticle shapes predicted by the cluster expansion have notable (116) facets. Based on the insights from the cluster expansion, we have used density functional theory to calculate the (116) surface energy. Our calculations indicate that the (116) surface is one of the lowest-energy surfaces for sodium alanate, suggesting that it may play an important role in hydrogen storage and release reactions.

Publications

1. Mueller, T. and Ceder, G., *An ab-initio study of the low-temperature phases of lithium imide*. Physical Review B, submitted (2009).

2. Mueller, T. and Ceder, G., *Bayesian approach to cluster expansions*. Physical Review B, submitted (2009).

3. Brandon Wood and Nicola Marzari, Dynamics and Thermodynamics of a Novel Phase of NaAlH4, Physical Review Letters, submitted (2009).

4. H. Gunaydin, K.N. Houk, and V. Ozolins, *"Kinetics of vacancy formation in $NaAlH_4$,"* in preparation (2009).

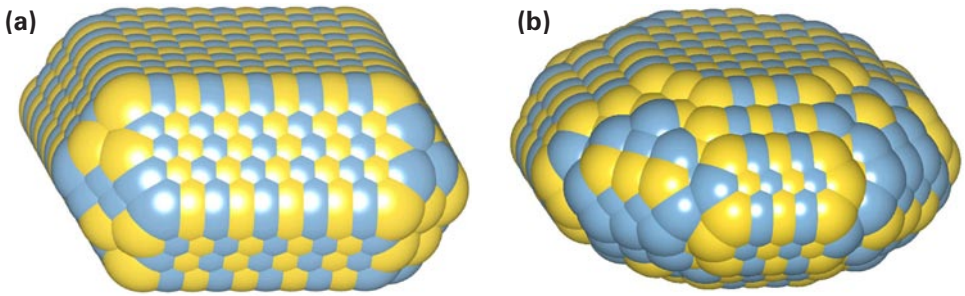

FIGURE 7. The predicted ground state shape of a $NaAlH_4$ nanoparticle predicted by (a) a Wulff construction, and (b) the cluster expansion method. Orange spheres represent Na, and blue sphere represent AlH_4 groups.

5. A. Akbarzadeh, C. Wolverton, and V. Ozolins, *"First-principles determination of crystal structures, phase stability, and reaction thermodynamics in the Li-Mg-Al-H hydrogen storage system,"* to appear in Physical Review B (2009).

6. H. Gunaydin, S.V. Barabash, K.N. Houk, and V. Ozolins, *"First-principles theory of hydrogen diffusion in aluminum,"* Physical Review Letters **101**, 075901 (2008).

7. E.H. Majzoub and V. Ozolins, *"Prototype electrostatic ground state approach to predicting crystal structures of ionic compounds: Application to hydrogen storage materials,"* Physical Review B **77**, 104115 (2008).

8. H. Gunaydin, K.N. Houk, and V. Ozolins, *"Vacancy mediated dehydrogenation of sodium alanate,"* Proceedings of the National Academy of Sciences USA (PNAS) **105**, 3673-3677 (2008).

9. M.J. Tambe, N. Bonini, and N. Marzari, *"Bulk aluminum at high pressure: A first-principles study,"* Physical Review B **77**, 172102 (2008).

Personnel

Gerbrand Ceder: Faculty
Nicola Marzari: Faculty
Vidvuds Ozolins: Faculty
Tim Mueller: Postdoctoral Associate
Hakan Gunaydin: Postdoctoral Associate
Sergey Barabash: Research Engineer
M. Tambe: Graduate Student
F. Baletto: Postdoctoral Associate
T. Thonhauser: Research Associate
B. Wood: Postdoctoral Researcher